7362 *Inorg. Chem.* **2010**, *49*, 7362–7371
DOI: 10.1021/ic100466s

Inorganic Chemistry
Article

Structural and Electronic Effects in the Metalation of Porphyrinoids. Theory and Experiment

Łukasz Orzeł,[†] Agnieszka Kania,[†] Dorota Rutkowska-Żbik,[‡] Anna Susz,[†,§] Grażyna Stochel,[*,†] and Leszek Fiedor[*,§]

[†]*Faculty of Chemistry, Jagiellonian University, Ingardena 3, 30-060 Kraków, Poland,* [‡]*Institute of Catalysis and Surface Chemistry, Polish Academy of Sciences, Niezapominajek 8, 30-239 Kraków, Poland, and* [§]*Faculty of Biochemistry, Biophysics and Biotechnology, Jagiellonian University, Gronostajowa 7, 30-387 Kraków, Poland*

Received March 10, 2010

The structure−reactivity relationships in metalation reactions of porphyrinoids have been studied using experimental and theoretical methods. A series of eight porphyrinoic ligands, derivatives of chlorophylls, was prepared in which both the peripheral groups and the degrees of saturation of the macrocycle were systematically varied. To reveal the solvent and structural factors which control the interactions of these macroligands with metal centers, their interactions with reactive Zn^{2+} and inert Pt^{2+} ions were investigated using absorption spectroscopy. In parallel, quantum chemical calculations (density functional theory, DFT) were performed for the same set of molecules to examine the influence of structural and electronic factors on the energy of the frontier orbitals, the nucleophilicity/electronegativity of the macrocycle, its hardness, and conformation. These static descriptors of chemical reactivity, relevant to metalation reactions, were verified against the results obtained in the experimental model. The experimentally obtained kinetic data clearly show that the solvent has a crucial role in the activation of the incoming metal center. In terms of chelator structure, the largest effects concern the size of the delocalized π-electron system and the presence of side groups. Both the DFT calculations and experimental results show the strong influence of the macrocycle rigidity and of the peripheral groups on the chelating ability of porphyrinoids. In particular, the peripheral functionalization of the macrocyclic system seems to drastically reduce its reactivity toward metal ions. The effect of peripheral groups is twofold: (i) a lower electron density on the core nitrogens, and (ii) increased rigidity of the macrocycle. The outcomes of the theoretical and experimental analyses are discussed also in terms of their relevance to the mechanism of biological metal insertion in the biosynthesis of heme and chlorophyll.

Introduction

Metalloporphyrinoids, in particular metallosubstituted derivatives of chlorophylls (Chls) have many characteristics as potent photosensitizers for triplet energy transfer, i.e., strong absorption maxima within the "therapeutic window" (>600 nm), high yields of triplet state, and efficient generation of $^1O_2$ and other reactive oxygen species. These features make them very interesting for therapeutic applications, for instance, in photodynamic therapy (PDT).[1−10] On the other hand, the metal exchange in Chls readily takes place in situ in plants grown in heavy metal-polluted soils, and metallosubstituted Chls have been found in lichens, microalgae, and water plants grown on media enriched in salts of these metals.[11−14] Because the central metal strongly influences the photophysical properties of chromophores,[15−19] the formation of

*To whom correspondence should be addressed. Fax: +48-12-6646902, E-mail: leszek.fiedor@uj.edu.pl (L.F.); Fax: +48-12-6340515, E-mail: stochel@chemia.uj.edu.pl (G.S.).

(1) Fiedor, J.; Fiedor, L.; Winkler, J.; Scherz, A.; Scheer, H. *Photochem. Photobiol.* **2001**, *74*, 64–71.
(2) Fiedor, L.; Gorman, A. A.; Hamblett, I.; Rosenbach-Belkin, V.; Salomon, Y.; Scherz, A.; Tregub, I. *Photochem. Photobiol.* **1993**, *58*, 506–511.
(3) Spikes, J. D.; Bommer, J. C. Chlorophyll and related pigments as photosensitizers in biology and medicine. In *Chlorophylls*; Scheer, H., Ed.; CRC Press: Boca Raton, FL, 1991; pp 1181−1196.
(4) Rosenbach-Belkin, V.; Chen, L.; Fiedor, L.; Salomon, Y.; Scherz, A. Chlorophyll and bacteriochlorophyll derivatives as photodynamic agents. In *Photodynamic Tumor Therapy. 2nd and 3rd Generation Photosensitizers*; Moser, J. G., Ed.; Harwood Academic Publishers: Amsterdam, The Netherlands, 1998; pp 117−125.
(5) Rosenbach-Belkin, V.; Chen, L.; Fiedor, L.; Tregub, I.; Pavlotsky, F.; Brumfeld, V.; Salomon, Y.; Scherz, A. *Photochem. Photobiol.* **1996**, *64*, 174–181.
(6) Bonnett, R. *Chem. Soc. Rev.* **1995**, *24*, 19–33.
(7) Bonnett, R. Metal complexes for photodynamic therapy. In *Comprehensive Coordination Chemistry*; McCleverty, J. A., Meyer, T. J., Eds.; Elsevier: Amsterdam, The Netherlands, 2003.
(8) Nyman, E. S.; Hynninen, P. H. *J. Photochem. Photobiol., B* **2004**, *73*, 1–28.
(9) Brandis, A. S.; Salomon, Y.; Scherz, A. Chlorophyll sensitizers in photodynamic therapy. In *Chlorophylls and Bacteriochlorophylls. Biochemistry, Biophysics, Functions and Applications*; Grimm, B., Porra, R. J., Rudiger, W., Scheer, H., Eds.; Springer: Dordrecht, The Netherlands, 2006; pp 462−483.
(10) Szaciłowski, K.; Macyk, W.; Drzewiecka-Matuszek, A.; Brindell, M.; Stochel, G. *Chem. Rev.* **2005**, *105*, 2647–2694.

 Published on Web 07/22/2010

complexes of heavy-metal ions (Hg, Cd, Ni, Cu, La, and Pb) with Chls leads to an impairment of the photosynthetic machinery.[11−14] Importantly for inevitable interactions of Chls derivatives with living organisms, the type of the central metal influences their pharmacokinetics.[20,21] Metalloporphyrinoids also receive considerable attention as model pigments in photosynthesis research and as the building blocks of supramolecular devices.[15,16,19,22−24]

Therefore, the interactions of porphyrinoids with metal ions are not only of theoretical interest. The metalation reactions of simpler porphyrins have been thoroughly discussed,[25−29] and en bloc, the mechanisms of metalation of porphyrins and pheophytins and the metal exchange in metalloporphyrins and Chls appear very similar, respectively. However, in the case of Chls a variety of additional factors have to be considered: differences in π-electron distribution, macrocycle rigidity/conformation, and the influence of peripheral groups make Chls prone to different effects, as indicated in earlier studies.[24,30−33] The presence of either one (in Chls) or two (in bacteriochlorophylls, BChls) reduced pyrrole rings, fusion with the isocyclic ring and some peripheral substituents, shape their electronic structure and in consequence also their reactivity and chelating properties. This is reflected, for instance, in the fact that (trans)metalation of Chls with many divalent metal ions occurs spontaneously under ambient conditions,[12,33−35] whereas that of BChls requires the application of synthetic methods.[15]

Many factors are known to influence the reactivity of tetrapyrroles, such as the nature of the solvent, the macrocycle conformation, the coordination of incoming metal ions, and the aggregation effects, particularly strong in metalloporphyrins with small peripheral substituents, as reviewed extensively.[36−38] The chemical reactivity of porphyrins and related molecules is also strongly determined by electronic and steric effects. The present study aims to establish the structure−reactivity relationships in interactions of divalent metal ions with functionalized derivatives of porphyrins, macroligands important from the synthetic and biological points of view. In order to obtain a comprehensive picture, two complementary approaches were applied: (1) a comparison of the reactivity of model pigments in chelation reactions with divalent metal ions of different reactivity, and (2) quantum chemistry calculations (density functional theory, DFT) of model pigments. To this end, a series of demetalated derivatives of Chla and BChla was prepared in which structural elements systematically vary. The modifications concern both the π-electron distribution over the tetrapyrrolic skeleton (number of reduced rings) and the peripheral substituents at the C-7, C-13^2, and C-17^3 sites (Scheme 1). The reactions were carried out with reactive Zn^{2+} and inert Pt^{2+} ions in two solvents, methanol (MeOH) and acetonitrile (MeCN). The same set of chelators, extended to also include structures of parental porphyrins, was chosen for the DFT calculations, carried out in order to correlate the experimental results with the predicted structural and electronic properties of the ligands relevant to metalation reactions.

Methods

Experimental Methods. Porphyrinoids. Chla was isolated from the cells of cyanobacterium *Arthrospira maxima* obtained from the Culture Collection of Autotrophic Organisms in Trebon (Czech Republic). The pigment was extracted in methanol according to Iriyama[39] and purified by column chromatography on DEAE-Sepharose (Sigma, Germany)[40] and then by isocratic reversed-phase high-performance liquid chromatography (HPLC) (Varian RP-C18, 250 × 10 mm, flow rate: 4 mL/min) using methanol as the eluent. The separations were run on an HPLC system consisting of a ProStar 230 pump (Varian, USA) equipped with a TIDAS diode array detector (J&M, Germany) for online monitoring of absorption spectra. BChla was isolated from the wet cells of *Rhodobacter sphaeroides* following a previously described method.[41] The pigment was purified by column chromatography on DEAE-Sepharose (Sigma, Germany)[42] and by HPLC on a semipreparative silica gel column (Varian).[41] Chlb was extracted from spinach in methanol according to Iriyama[39] and separated from Chla using column chromatography on Sepharose CL-6B using 10%

(11) Scheer, H. The pigments. In *Light Harvesting Antenas in Photosynthesis*; Green, B., Parson, W., Eds.; Kluwer Academic Publishers: Dordrecht, The Netherlands, 2003; pp 29−81.
(12) Küpper, H.; Küpper, F.; Spiller, M. *J. Exp. Bot.* **1996**, *47*, 259–266.
(13) Küpper, H.; Küpper, F.; Spiller, M. *Photosynth. Res.* **1998**, *58*, 123–133.
(14) Küpper, H.; Setlik, I.; Spiller, M.; Küpper, F.; Prasil, O. *J. Phycol.* **2002**, *38*, 429–441.
(15) Hartwich, G.; Fiedor, L.; Simonin, I.; Cmiel, E.; Schafer, W.; Noy, D.; Scherz, A.; Scheer, H. *J. Am. Chem. Soc.* **1998**, *120*, 3675–3683.
(16) Noy, D.; Fiedor, L.; Hartwich, G.; Scheer, H.; Scherz, A. *J. Am. Chem. Soc.* **1998**, *120*, 3684–3693.
(17) Musewald, C.; Hartwich, G.; Lossau, H.; Gilch, P.; Poellinger-Dammer, F.; Scheer, H.; Michel-Beyerle, A. E. *J. Phys. Chem. B* **1999**, *103*, 7055–7060.
(18) Musewald, C.; Hartwich, G.; Poellinger-Dammer, F.; Lossau, H.; Scheer, H.; Michel-Beyerle, A. E. *J. Phys. Chem. B* **1998**, *102*, 8336–8342.
(19) Drzewiecka-Matuszek, A.; Skalna, A.; Karocki, A.; Stochel, G.; Fiedor, L. *J. Biol. Inorg. Chem.* **2005**, *10*, 453–462.
(20) Szczygieł, M.; Urbańska, K.; Jurecka, P.; Stawoska, I.; Stochel, G.; Fiedor, L. *J. Med. Chem.* **2008**, *51*, 4412–4418.
(21) Dandler, J.; Wilhelm, B.; Scheer, H. *Photochem. Photobiol.* **2010**, *86*, 182–193.
(22) Yerushalmi, R.; Ashur, I.; Scherz, A. Metal-substituted bacteriochlorophylls: novel molecular tools. In *Chlorophylls and Bacteriochlorophylls. Biochemistry, Biophysics, Functions and Applications*; Grimm, B., Porra, R. J., Rudiger, W., Scheer, H., Eds.; Springer: Dordrecht, The Netherlands, 2006; Vol. *25*, pp 495−506.
(23) Yerushalmi, R.; Noy, D.; Baldridge, K. K.; Scherz, A. *J. Am. Chem. Soc.* **2002**, *124*, 8406–8415.
(24) Kania, A.; Fiedor, L. *J. Am. Chem. Soc.* **2006**, *128*, 454–458.
(25) Lavallee, D. K. *Coord. Chem. Rev.* **1985**, *61*, 55–96.
(26) Hambright, P. *Coord. Chem. Rev.* **1971**, *6*, 247–268.
(27) Hambright, P. Chemistry of water soluble porphyrins. In *The Porphyrin Handbook*; Kadish, K., Smith, K., Guilard, G., Eds.; Academic Press: New York, 1999; Vol. *3*, pp 121−210.
(28) Longo, F. R.; Brown, E. M.; Rau, W. G.; Adler, A. D. Kinetic and mechanistic studies of metalloporphyrin formation. In *The Porphyrins*; Academic Press: New York, 1978; Vol. *5* (Part C), pp 459−481.
(29) Tanaka, M. *Pure Appl. Chem.* **1983**, *55*, 151–158.
(30) Strell, M.; Urumow, T. *Liebigs Ann. Chem.* **1977**, 970–974.
(31) Fiedor, L.; Kania, A.; Myśliwa-Kurdziel, B.; Orzeł, Ł.; Stochel, G. *Biochim. Biophys. Acta, Bioenerg.* **2008**, *1777*, 1491–1500.
(32) Fiedor, L.; Stasiek, M.; Myśliwa-Kurdziel, B.; Strzałka, K. *Photosynth. Res.* **2003**, *78*, 47–57.
(33) Orzeł, Ł.; Fiedor, L.; Kania, A.; Wolak, M.; van Eldik, R.; Stochel, G. *Chem.—Eur. J.* **2008**, *14*, 9419–9430.
(34) Schunck, E.; Marchlewski, L. *Liebigs Ann. Chem.* **1894**, *278*, 329–345.
(35) Hynninen, P. H. Chemistry of chlorophylls: modifications. In *Chlorophylls*, Scheer, H., Ed.; CRC Press: Boca Raton, FL, 1991; pp 145−209.
(36) Smith, K. M. *Porphyrins and Metalloporphyrins*; Elsevier: Amsterdam, The Netherlands, 1975.
(37) Dolphin, D. *The Porphyrins*: Academic Press: New York, 1978.
(38) Kadish, K. M.; Smith, K. M.; Guilard, R. *The Porphyrin Handbook*; Academic Press: Amsterdam, The Netherlands, 1999.
(39) Iriyama, K.; Ogura, N.; Takamiya, A. *J. Biochem.* **1974**, *76*, 901–904.
(40) Omata, T.; Murata, N. *Plant Cell Physiol.* **1983**, *24*, 1093–1100.
(41) Fiedor, L.; Rosenbach-Belkin, V.; Scherz, A. *J. Biol. Chem.* **1992**, *267*, 22043–22047.
(42) Omata, T.; Murata, N. *Photochem. Photobiol.* **1980**, *31*, 183–185.

Scheme 1. Structures of Free Bases Studied in Metalation Reactions with Zn^{2+} and Pt^{2+} Ions: $13^2(S)$-Pheophytin *a* (**I**), $13^2(R)$-Pheophytin *a* (**II**), $13^2(S)$-Hydroxypheophytin *a* (**III**), $13^2(S)$-Pheophorbide *a* (**IV**), $13^2(S)$-3-Acetylpyropheophytin *a* (**V**), $13^2(S)$-Pheophytin *b* (**VI**), $13^2(S)$-Bacteriopheophytin *a* (**VII**), and $13^2(S)$-Bacteriopheophorbide *a* (**VIII**)[a]

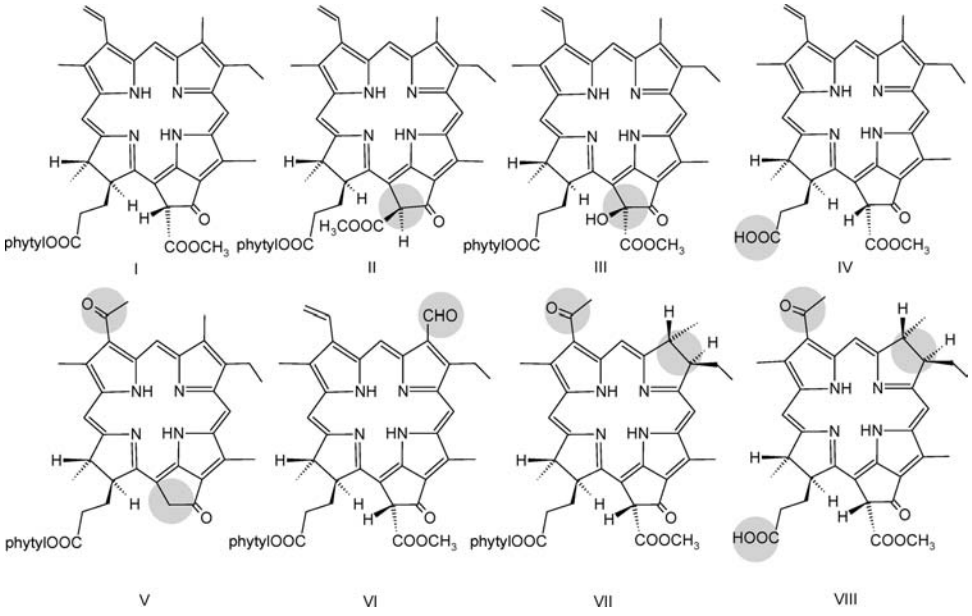

[a] Grey circles indicate the sites of modifications.

2-propanol in *n*-hexane as the eluent. The final purification was done by isocratic reversed-phase HPLC using neat methanol (Varian RP C-18, 250 × 10 mm, flow rate: 4 mL/min). In all cases, only the fractions of pure diastereisomeric forms of the pigments were collected.

Chlorophyllides (the $13^2(S)$-diastereisomers) were obtained via enzymatic hydrolysis of Chla and BChla, respectively, using the plant enzyme chlorophyllase obtained from the leaves of *Fraxinus excelsior* following a previously described procedure.[41] The products were purified twice by column chromatography on CM-Sepharose (Pharmacia, Sweden) as described earlier.[41] The 13^2-hydroxy-Chla and 3-acetyl-pyro-Chla were a kind gift from Prof. Hugo Scheer (LMU München, Germany). Their purity (single bands, not shown) was confirmed by thin-layer chromatography (TLC) analysis on silica gel (TLC Silica gel 60, Merck), as described previously.[41]

Pheophytins (**I**−**III** and **V**−**VII**, structures shown in Scheme 1) and pheophorbides (**IV** and **VIII**) were prepared from the corresponding purified magnesium complexes by a short treatment with a small amount of doubly distilled glacial acetic acid at room temperature, as described earlier.[41] The acid was removed in a stream of nitrogen, and the product was dried under vacuum and quickly purified by column chromatography either on DEAE-Sepharose in acetone (**I**−**III** and **V**−**VII**) or on CM-Sepharose (**IV** and **VIII**). The purity of the pigments was confirmed by the reversed-phase HPLC (not shown). Only freshly prepared pigments were used for the reactions, and samples showing signs of allomerization or oxidation were discarded. Tetracarboxyphenylporphyrin (TCPP) and protoporphyrin IX (PPIX) were purchased from Frontier Scientific (USA). All preparative steps were done as quickly as possible and under dim light.

Metalation Reactions. Zinc Insertion. All reactions of **I**−**VIII** with zinc trifluoromethanesulfonate ($ZnTf_2$) in MeOH and MeCN were carried out at 298 K. In order to maintain pseudo-first-order conditions, the concentration of $ZnTf_2$ was varied between 0.5 and 5.0 mM, whereas the concentration of tetrapyrrolic ligands was kept constant at 2.5 μM. The kinetics of individual reactions of **I**−**VIII** were followed at the maxima of the Q_Y band of both the substrates and the products, as shown in Figure 1. The course of reactions was also monitored by performing TLC analysis on silica gel, as described above (not shown).

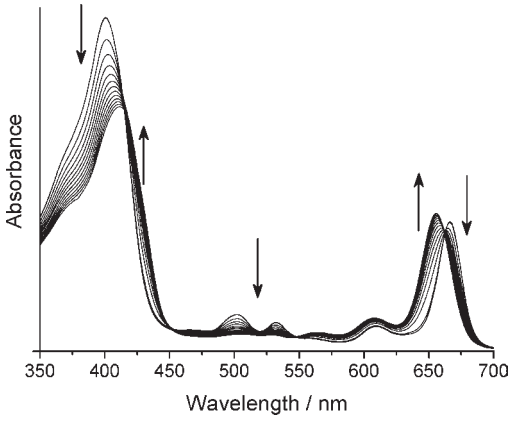

Figure 1. Spectral changes accompanying metalation of pheophytins. As an example, the reaction of 13^2-hydroxypheophytin *a* (**III**) with $ZnTf_2$ in MeOH is shown. [**III**] = 2.5 μM, [$ZnTf_2$] = 5 mM, T = 298 K. Spectra were recorded every 60 min. The arrows indicate the direction of changes occurring during the reaction.

Platinum Insertion. $K_2[PtCl_4]$ was used as the source of Pt^{2+} ions in metalations of pheophytins **I**, **III**, **IV**, **V**, and **VI**. The solution of $K_2[PtCl_4]$ (5 mg) in 0.1 mL of water was added to 1 mL of glacial acetic acid containing the pigment (1 mg) and CH_3COONa (30 mg). The metalations were carried out at room or elevated temperature under dim light. The course of reactions was monitored by performing TLC analysis on silica gel and by recording the electronic absorption spectra of aliquots (25 μL) of reaction mixtures dissolved in 2 mL MeOH.

Reagents. Methanol, *n*-hexane, and 2-propanol were of HPLC grade (LabScan, Ireland). Acetone and 1,4-dioxane were of analytical grade (POCh, Poland). Glacial acetic acid (POCh, Poland), before use, was distilled twice in the presence of solid $KMnO_4$. MeCN and MeOH used in kinetic measurements were of spectroscopic grade (Lach-Ner s.r.o., Czech Republic).

All solvents were degassed under vacuum prior to use. $ZnTf_2$ was purchased from Sigma-Aldrich (Germany).

Spectroscopic Studies. The reactions of pheophytins with $ZnTf_2$ in MeOH and MeCN were carried out in quartz 0.88 cm tandem cuvettes and followed by electronic absorption spectroscopy using a Lambda 35 (Perkin-Elmer, U.K.) spectrophotometer equipped with a PTP-6 Peltier temperature controller (Perkin-Elmer, U.K.). Other electronic absorption spectra were recorded on a Cary 400 spectrophotometer (Varian, U.S.A.) in 1 cm quartz cuvettes at room temperature.

Computational Methods. The electronic and fully optimized geometric structures of free base porphyrin, chlorin, and bacteriochlorin, the corresponding 13^1-oxo-phorbin analogs, and the target ligands **I**−**VIII** were obtained within the DFT method applying the Becke−Perdew fuctional,[43,44] as implemented in the Turbomole package (version 5.8, Turbomole GmbH, Germany) according to methods described previously.[45,46] The Resolution-of-Identity (RI) approach was applied for computing the electronic Coulomb interactions.[47] For all atoms, the TZVP quality basis sets were applied.[47,48]

Results and Discussion

Choice of Model System. To test the effects of specific structural features on the reactivity of tetrapyrrolic ligands toward metal ions, a series of model tetrapyrrolic ligands **I**−**VIII** (structures shown in Scheme 1), derivatives of Chla (**I**−**VI**) and BChla (**VII** and **VIII**), was prepared. The sensitivity of their absorption spectra to chelation facilitated an easy and direct monitoring of the metalation reaction progress. The ability of model ligands **I**−**VIII** to form chelates was studied in reactions with Zn^{2+} and Pt^{2+} which are divalent metal ions of different reactivities in metalation reactions. Under ambient conditions, the Zn^{2+} ion is reactive and spontaneously inserts into most of the model free bases, while the Pt^{2+} ion is rather nonreactive, and its insertion requires activating conditions (see below). Importantly, the two metal ions do not readily change their redox state under the conditions of the metalation reaction. The metalations were carried out in MeOH and in MeCN, chosen as good solvents for both reactants, i.e., for the pigments and sources of metal ions. To prevent the allomerization of the pigments, the solvents were degassed prior to use, and the cuvettes in which the measurements were performed were sealed under Ar. In the absence of metal ions, no degradation of pigments was observed in these solvents in the time scale of the experiment, if judged by the absence of shifts in the absorption spectra and by TLC analysis (not shown). To avoid interactions of the Zn^{2+} ion with extra ligands, a noncoordinating triflate (Tf) was chosen as its counterion. In order to achieve the activation of Pt^{2+} ion, its reactions with **I**−**VIII** were carried out in concentrated acetic acid (HAc) at ambient and increased temperatures.

Regarding **I** (pheophytin a) as the reference ligand, the following structural modifications were applied along the series of model porphyrinoids:

- **II.** Configuration inversion at C-13^2.
- **III.** Hydroxylation at C-13^2.
- **IV.** Removal of phytyl chain, leaving a free carboxyl group.
- **V.** Introduction of acetyl at C-3 and removal of methoxycarbonyl at C-13^2.
- **VI.** Introduction of a formyl group at C-7.
- **VII.** Reduction of C=C bond in ring II and introduction of acetyl at C-3.
- **VIII.** Reduction of C=C bond in ring II, introduction of acetyl at C-3, and removal of phytyl chain, leaving a free carboxyl group.

Metalation Reactions and Their Kinetics. The progress of the chelation of the Zn^{2+} ion by free bases **I**−**VIII** was followed using absorption spectroscopy. A typical pattern of changes in the absorption spectrum of the reaction mixture, occurring during the reactions of **I**−**VI** with $ZnTf_2$, is seen in Figure 1 in which the reaction with **III** is shown as an example.

The addition of $ZnTf_2$ to the solutions of chlorin derivatives **I**−**VI** in MeOH or MeCN causes a considerable (∼10 nm) blue shift of the Q_Y band. Simultaneously, weak bands between 500 and 550 nm disappear, and the shape of the Soret band changes. The isosbestic points near 450, 550, and 660 nm (Figure 1) indicate that no stable intermediates are formed in the time scale of the experiment. The spectral shifts accompanying the reactions of BChla derivatives, **VII** and **VIII**, with $ZnTf_2$ in both solvents were different (Figure S1 in Supporting Information). Initially (3−4 h), a small red shift of the Q_Y band could indicate some interactions of the ligands with Zn^{2+} ion, but at longer periods, the band bleached and was accompanied by the appearance of new bands near 680 and 430 nm. Such changes are indicative of the oxidation of **VII** and **VIII** to a chlorin type of pigment,[49] and because they do not relate to metal insertion, their kinetics were not studied further.

In kinetic experiments, the concentration of model chelators was kept constant at 2.5 μM, whereas [Zn^{2+}] (as $ZnTf_2$) was varied from 0.5 to 5.0 mM. A large excess of Zn^{2+} ions over the free base was applied in order to secure pseudofirst-order conditions. The rates of metalation showed a strong solvent dependence, as at 298 K, the reactions of **I**−**VI** with $ZnTf_2$ in MeCN were completed within minutes and within several hours in MeOH (Table 1). The half-times of metalation ($\tau_{1/2}$) of **I**−**V** were comparable (∼2 h), while that of **VI** was considerably longer (6 h).

Except for the reaction with **I** in MeCN, where a double-exponential course was observed, the kinetic traces obtained for the formation of the Zn complexes reveal a clear monoexponential course. Hence, a monoexponential fitting of the kinetic traces for **I**−**VI** in MeOH as well as for **II**−**VI** in MeCN provided the values of k_{obs}, whereas a double-exponential fitting applied for **I** in MeCN provided the k_{obs} and k_{obs}' values. The latter

(43) Becke, A. D. *Phys. Rev. A: At., Mol., Opt. Phys.* **1988**, *38*, 3098–3100.
(44) Perdew, J. P. *Phys. Rev. B: Condens. Matter Mater. Phys.* **1986**, *33*, 8822–8824.
(45) Rodakiewicz-Nowak, J.; Nowak, P.; Rutkowska-Żbik, D.; Ptaszek, M.; Michalski, O.; Mynarczuk, G.; Eilmes, J. *Supramol. Chem.* **2005**, *17*, 643–647.
(46) Rutkowska-Zbik, D.; Witko, M. *J. Mol. Catal. A: Chem.* **2006**, *258*, 376–380.
(47) Koga, T.; Kobayashi, H. *J. Chem. Phys.* **1985**, *82*, 1437–1439.
(48) Helgaker, T. *Chem. Phys. Lett.* **1991**, *182*, 503–510.
(49) Lindsay, J. S.; Mauzerall, D. C. *J. Am. Chem. Soc.* **1982**, *104*, 4498–4500.

Table 1. Kinetic Parameters for the Reactions of Chlorophyll Derivatives (Free Bases) **I**−**VI** with $ZnTf_2$ in Organic Solvents MeOH and MeCN[a]

	$\tau_{1/2}$[b]		k_{obs} [s^{-1}][b]		k_1 [$M^{-1}s^{-1}$]		k_2 [s^{-1}]	
ligand	MeOH	MeCN	MeOH	MeCN	MeOH	MeCN	MeOH	MeCN
I	2 h	1 min	1.14×10^{-4}	1.04×10^{-2}	$8.8 \pm 1.3 \times 10^{-3}$	2.6 ± 0.1	$7.1 \pm 0.4 \times 10^{-5}$	$3.8 \pm 0.3 \times 10^{-1}$[c]
II	2.6 h	1 min	7.53×10^{-5}	1.21×10^{-2}	$6.6 \pm 0.5 \times 10^{-3}$	2.2 ± 0.1	$4.3 \pm 0.2 \times 10^{-5}$	$1.1 \pm 0.4 \times 10^{-3}$
III	2.2 h	5 min	9.46×10^{-5}	2.04×10^{-3}	$7.5 \pm 1.2 \times 10^{-3}$	$3.9 \pm 0.1 \times 10^{-1}$	$5.7 \pm 0.4 \times 10^{-5}$	$1.5 \pm 0.3 \times 10^{-4}$
IV	2 h	2 min	1.10×10^{-4}	5.50×10^{-3}	$1.1 \pm 0.1 \times 10^{-2}$	$7.5 \pm 0.6 \times 10^{-1}$	$5.4 \pm 0.2 \times 10^{-5}$	$1.5 \pm 0.2 \times 10^{-3}$
V	2.2 h	1 min	8.36×10^{-5}	1.23×10^{-2}	$7.3 \pm 0.4 \times 10^{-3}$	1.7 ± 0.1	$4.7 \pm 0.1 \times 10^{-5}$	$2.2 \pm 0.2 \times 10^{-3}$
VI	6 h	5 h	3.29×10^{-5}	1.01×10^{-4}	$4.2 \pm 0.2 \times 10^{-3}$	$1.4 \pm 0.1 \times 10^{-2}$	$1.2 \pm 0.1 \times 10^{-5}$	$3.3 \pm 0.1 \times 10^{-5}$

[a] All parameters were determined at 298 K. For simplicity, k_1' is represented by k_2 (see the text for details). [b] $[ZnTf_2] = 5$ mM. [c] In $[M^{-1}s^{-1}]$.

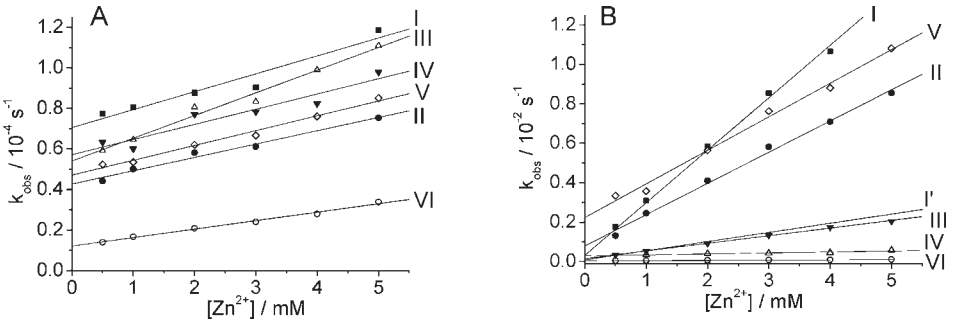

Figure 2. Dependence of the rate constants of metalation of free bases **I**−**VI** on the concentration of Zn^{2+} ions in MeOH (A) and MeCN (B). **I** and **I′** in panel B relate to the parallel processes observed in the reaction of **I**, $T = 298$ K and [free base] $= 2.5\ \mu$M.

two parameters most likely correspond to two parallel processes involving two reactive species of Zn^{2+} (different coordinative forms) in MeCN. The relationships between k_{obs} and $[Zn^{2+}]$ show a linear character with intercepts more distinct in MeOH than in MeCN (compare Figure 2A and B).

Thus, the common rate law, viz.:

$$k_{obs} = k_1[Zn^{2+}] + k_2 \quad (1)$$

in which k_1 and k_2 are inferred from the slopes and intercepts from the plots of k_{obs} against $[Zn^{2+}]$, respectively, and can be applied to describe the kinetics of reactions of **I**−**VI** in MeOH and of **II**−**VI** in MeCN. In the case of **I** in MeCN, the intercepts in the plots of k_{obs} and k_{obs}' vs $[Zn^{2+}]$ were negligible, and thus the respective rate laws simplify to

$$k_{obs} = k_1[Zn^{2+}] \quad (2)$$

and

$$k_{obs}' = k_1'[Zn^{2+}] \quad (2')$$

Many reports on the metalation of tetrapyrrolic ligands refer to a variety of rate laws.[25−28,50,51] Commonly, a linear relationship has been applied, analogous to eq 1, but Tanaka et al. showed that the form of the rate law markedly depends on the concentration of the incoming metal ion.[52] With increasing concentration, the linear relationship turns into a hyperbolic one:

$$k_{obs} = \frac{k_1K[M^{2+}]}{1 + K[M^{2+}]} \quad (3)$$

in which K corresponds to a fast pre-equilibrium that precedes the rate limiting step, defined by k_1. The pre-equilibrium refers to the formation of an initial metal ion−macrocycle adduct held together by weak electrostatic interactions. A similar saturation kinetic law has been suggested previously for the metalation of porphyrins[29,52] and also applied in our recent study to describe the kinetics of Cu^{2+} insertion into **I** in MeCN.[53] In some cases, the plots of k_{obs} vs $[Zn^{2+}]$ for the reaction in MeCN provide a slight indication of saturation that could be reached at higher concentrations of the Zn^{2+} ion but inaccessible in this solvent. Nevertheless, the apparent curvatures are even less pronounced than in reactions with Cu^{2+} ion,[53] and the linear rate law (eqs 1, 2, and 2′) can be satisfactorily assumed in the present kinetic description.

Generally, the k_2 parameter in eq 1 may refer either to a backward or a parallel reaction, but in the case of the Zn−Chla formation, the former possibility seems less reasonable because, once formed, the complex is very stabile. Therefore, the occurrence of two parallel metalation processes appears more convincing as the explanation of k_2. A similar interpretation of this free parameter was assumed for the formation of Cu−Chla in both MeOH and MeCN.[53] Thus, either the metal ion reacts with two species of the free base (e.g., **I** and traces of its

(50) Fleischer, E. B.; Choi, E. I.; Hambright, P.; Stone, A. *Inorg. Chem.* **1964**, *3*, 1284–1287.
(51) Berezin, B. D.; Smirnova, G. I. *Russ. J. Phys. Chem.* **1967**, *41*, 702–705.
(52) Funahashi, S.; Yamaguchi, Y.; Tanaka, M. *Bull. Chem. Soc. Jpn.* **1984**, *57*, 204–208.
(53) Orzeł, Ł.; van Eldik, R.; Fiedor, L.; Stochel, G. *Eur. J. Inorg. Chem.* **2009**, 2393–2406.

allomer **III**) or, more likely, the free base reacts with two species (coordinative forms) of metal ion. As triflate is only weakly coordinating, the interactions of Zn^{2+} ions with water and other trace impurities of MeOH cannot be excluded. Nevertheless, one can interpret the [Zn^{2+}]-dependent k_1' and the [Zn^{2+}]-independent k_2 as the rate constants applying to the same type of parallel reactions which involves minor coordinative forms of Zn^{2+} ion present in reaction mixtures, e.g., coordinating counterions or trace water molecules. The kinetic parameters obtained for all reactions in MeOH and MeCN are summarized in Table 1 (in which, for simplicity, k_1' is indicated under k_2). As mentioned above, the contributions of k_2 values to the overall reaction rates are insignificant, especially in MeCN, and therefore only k_1 values are considered in further discussion.

A comparison of the kinetic data for the insertion of Zn^{2+} carried out in MeOH and MeCN (Table 1) points at the crucial role of the solvent. The metalation of free bases **I**−**V** is approximately two orders of magnitude faster in MeCN than in MeOH. Several reasons for such a solvent effect have to be considered. Because the rate-determining step in the metalation is the formation of the first coordinative bond between an incoming metal ion and a free core nitrogen, occurring prior to deprotonation of the next nitrogen atom,[54] the hydrogen-bond (H-bond) donating/accepting properties of the solvent are of importance. Protic solvent molecules can H-bond to the periphery and/or to the core of the tetrapyrrolic ligand and thus affect its reactivity toward metal ion. For instance, protonation of the C-13[1] carbonyl shifts the keto−enol equilibrium and labilizes protons on the pyrrolenine nitrogens, which in turn speeds up the insertion of the metal ion.[15] The effects of protonation at the C-13[1] site are significant only in acidic media (e.g. acetic acid)[15] and will not play a role in neutral solvents, such as MeOH and MeCN. More likely, MeOH weakly H-bonds to the pyrrolenine nitrogens which inhibits free base−Zn^{2+} interactions.[55,56] On the other hand, a more nucleophilic MeCN is expected to slightly activate the free base by pulling the protonated core nitrogens out of the plane thus exposing the electron pairs of the nonprotonated nitrogens to the incoming metal ion. Furthermore, the coordinative properties of MeOH are considerably stronger than those of MeCN (solvent donor numbers 30 and 14, respectively), and hence the complexes of MeOH with Zn^{2+} ions are more stable. Indeed, the differences between **I**−**V** with respect to the rates of their metalation are minimized in MeOH. In the case of **VI**, the effect of a strongly electron-withdrawing −CHO group is dominant (see below), and a very weak solvent effect is observed. The involvement of various coordinative forms of the incoming metal ions in the metal insertion reactions will be a subject of another manuscript.

The variation in the values of $\tau_{1/2}$ and rate constants in MeCN is noticeably larger than in MeOH. In MeCN, **VI** is also least reactive, reaching $\tau_{1/2}$ values over 1 order of magnitude larger than in the reactions of **I**−**V,** while the reaction of **III** is 3−5 times slower than the metalations of **I**, **II**, and **V**.

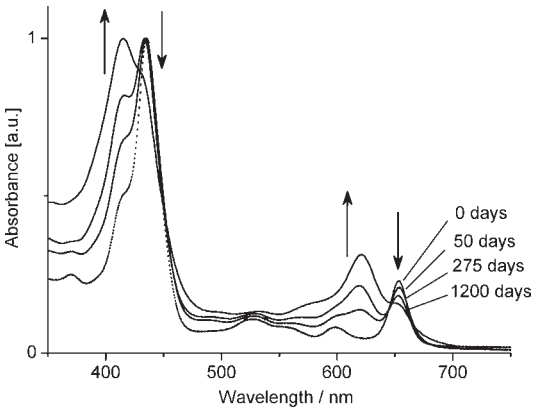

Figure 3. Spectral changes accompanying the insertion of Pt(II) ion into pheophytin b (**VI**). The reaction, carried out in MeOH at ambient temperature in a quartz cuvette sealed under Ar in the dark, is continuously monitored for over three years. The arrows indicate the direction of changes occurring during the reaction.

To gain additional information about the structure−reactivity relationship in tetrapyrrolic ligands, the metalation with Zn^{2+} was carried out with two simpler porphyrins, PPIX and TCPP. As an example, changes in the absorption spectrum that accompany the Zn^{2+} insertion into TCPP are shown in Figure S2 in the Supporting Information. Under conditions similar to those applied for the reactions of **I**−**VIII**, the k_{obs} of the metalation of both porphyrins (in MeOH) was near 2.5×10^{-4} s^{-1}, comparable to the k_{obs} values for the formation of Zn−Chls.

Insertion of Pt^{2+} into **I** and its derivatives is much more difficult than that of Zn^{2+}. The metalation, using K_2-[$PtCl_4$] as the source of Pt^{2+} ions and under activating conditions (concentrated acetic acid), proceeds very slowly at room temperature. Thus, the reaction of **I** was completed in about 35 days, while **V** needs 60 days to form the metalated complex. The reactions with **IV** and **VI** are even slower; being monitored for already about 150 and 1200 days, respectively, they are still incomplete (Figure 3). The insertion of Pt^{2+} can be accelerated by heating to 80 °C.[19,57] Even so, reaction does not take place with **VII** and **VIII**, although many combinations of experimental conditions were tested, i.e., a variety of solvents: acetic acid, dimethylformamide, and benzonitrile and sources of Pt^{2+} ions: K_2[$PtCl_4$], Pt(acac)$_2$, $PtCl_2$, and $(CH_3CN)_2$-$PtCl_2$ (not shown).

Theoretical Prediction of Chelating Properties of Chlorophylls. Three series of computations at the DFT level were performed in order to reveal the electronic structure−reactivity (nucleophilic properties) relationships in insertion of divalent metallic centers into model porphyrinoids. The optimized structures were characterized in terms of the charges on pyrrolenine nitrogen atoms, highest occupied molecular orbital (HOMO) and lowest unoccupied molecular orbital (LUMO) energies, the HOMO−LUMO energy gap, Mulliken's electronegativity (χ), and the hardness of the ligands (η). The results of computations are

(54) Inada, Y.; Sugimoto, Y.; Nakano, Y.; Itoh, Y.; Funahashi, S. *Inorg. Chem.* **1998**, *37*, 5519–5526.
(55) Berezin, B. D.; Smirnova, G. I. *Russ. J. Phys. Chem.* **1967**, *41*, 1271–1272.
(56) Berezin, B. D.; Smirnova, G. I. *Russ. J. Phys. Chem.* **1968**, *42*, 1026–1029.
(57) Macquet, J. P.; Theophanides, T. *Can. J. Chem.* **1973**, *51*, 219–226.

Table 2. Electronic Properties of Tetrapyrrolic Ligands Obtained in DFT Calculations

ligand	Loewdin charges on *N*	HOMO	LUMO	gap [eV]	χ	η
porphyrin	−0.06; −0.19; −0.06; −0.19	−5.09	−3.15	1.94	4.12	0.97
chlorin	−0.07; −0.14; −0.07; −0.20	−4.89	−3.09	1.80	3.99	0.90
bacteriochlorin	−0.08; −0.14; −0.08; −0.14	−4.44	−3.03	1.41	3.74	0.70
13^1-oxo-phorbin	−0.06; −0.13; −0.07; −0.20	−5.19	−3.51	1.68	4.35	0.84
13^1-oxo-bacteriophorbin	−0.06; −0.13; −0.08; −0.15	−4.78	−3.42	1.36	4.10	0.68
I	−0.05; −0.12; −0.06; −0.20	−5.05	−3.46	1.59	4.25	0.79
II	−0.05; −0.12; −0.06; −0.20	−5.03	−3.44	1.59	4.23	0.79
III	−0.05; −0.12; −0.06; −0.20	−5.09	−3.49	1.60	4.29	0.80
IV	−0.05; −0.12; −0.06; −0.20	−5.06	−3.47	1.59	4.26	0.79
V	−0.05; −0.12; −0.05; −0.20	−5.22	−3.68	1.54	4.45	0.77
VI	−0.05; −0.12; −0.06; −0.18	−5.29	−3.62	1.67	4.45	0.83
VII	−0.05; −0.12; −0.06; −0.14	−5.00	−3.73	1.27	4.36	0.63
VIII	−0.05; −0.12; −0.06; −0.14	−4.85	−3.66	1.19	4.25	0.59

summarized in Table 2. The first step of calculations consisted of geometry optimization of bare porphyrin, chlorin, and bacteriochlorin (none of them bearing an isocyclic ring). Then, the structures of 13^1-oxo-phorbin and 13^1-oxo-bacteriophorbin were built and fully reoptimized. Such a procedure enabled the comparison between the resulting geometries of chlorin and 13^1-oxo-phorbin and, similarly, bacteriochlorin and 13^1-oxo-bacteriophorbin. The basic structures of free base porphyrin, chlorin, and bacteriochlorin were compared in terms of the dependence of reactivity descriptors on the shape and the size of the π-electronic system. Next, the changes in ligand electronic structure induced by the isocyclic cyclopentanone ring were examined, and the resulting 13^1-oxo-phorbin analogs were taken as references structures for **I**−**VIII**. Finally, the complete structures of free bases **I**−**VIII** were compared in order to examine the effects of finer structural features on the ligand properties.

In general, several factors determine the reactivity of species in chemical reactions. The energy of the frontier orbitals (HOMO and LUMO), a common descriptor of chemical reactivity, and the match (in terms of shape and energy) between the frontier orbitals of the interacting species are among the key factors which control the reaction rate. In the case of porphyrins and their derivatives, in particular in reactions with metal ions, the nucleophilicity/electronegativity of the macrocycle, the hardness, and the conformation of the free base also have to be taken into consideration. The present theoretical analysis focuses on these "static" descriptors of the chemical reactivity of porphyrin derivatives. Any discussion of the kinetic factors would require another, obviously more elaborate approach, to account for the energetic and dynamic aspects of the metalation process. That is why only these static determinants of chemical reactivity will be here discussed in more detail.

The geometric parameters calculated for porphyrin, chlorin, and bacteriochlorin show that their macrocycles are planar with protons located in plane and with N−H bond lengths of about 1.02 Å, in line with the common notion that such extended aromatic systems are planar when no geometric constrains are present. As the pyrrole rings become saturated along the porphyrin−chlorin−bacteriochlorin row, the nucleophilicity of the macrocycle, expressed as molecular charges (Loewdin charges, Table 2) accumulated on the core nitrogens, is reduced. Concomitantly, the energy of the HOMO grows faster than that of the LUMO, resulting in a narrower gap, in agreement with previous studies.[58,59] At the same time, both the electronegativity and hardness of the macrocycle increase as follows: bacteriochlorin < chlorin < porphyrin.

The macrocycles of the 13^1-oxo-phorbin analogs are still planar, and molecular charges accumulated on the core nitrogens are only slightly reduced (Table 2), while the HOMO and LUMO energy levels appear by far more sensitive to the modification. The energies of both frontier orbitals are shifted downward with respect to basic chlorin and bacteriochlorin, resulting in a higher electronegativity. However, the HOMO−LUMO separation in the 13^1-oxo-phorbins is smaller and so is their hardness.

The side substituents affect both the electronic structure and the geometry of the tetrapyrrolic ligands. First, the planar conformation is retained in none of **I**−**VIII**; some carbon atoms move out-of-plane, leading to a slight ruffling, whereas the core nitrogens remain in plane. The ruffling should be attributed to steric interactions between the peripheral substituents, which is a general feature of sp^3-hybridized carbon atoms. This nonplanarity is particularly obvious in **II**, where it results from the repulsion between the phytyl chain and the methoxycarbonyl at C-13^2. Indeed, steric effects involving phytyl moiety have been experimentally shown to influence the coordinative and spectral properties of (B)Chls.[24,31,32]

In terms of HOMO and LUMO energies, free bases **I**−**VIII** can be separated into three groups: one consisting of **I**−**IV**, the second of **V** and **VI**, and the third of **VII** and **VIII** (Table 2), in agreement with the spectral properties of ground-state molecules. In all structures, HOMOs and LUMOs are localized on the atoms forming the macrocycle, in line with previous theoretical studies.[58,60−65] The peripheral groups induce shifts in the HOMO and LUMO levels and further affect the π-electron distribution around the macrocycle, as reflected in changes of charge density on core nitrogens. Thus, nitrogen atoms in

(58) Hanson, L. K. Molecular orbital theory of monomer pigments. In *Chlorophylls*; Scheer, H., Ed.; CRC Press: Boca Raton, FL, 1991; pp 993−1012.
(59) Ghosh, A. *J. Phys. Chem. B* **1997**, *101*, 3290–3297.
(60) Gouterman, M. *J. Mol. Spectrosc.* **1961**, *6*, 138–163.
(61) Shelnutt, J. A.; Ortiz, V. *J. Phys. Chem.* **1985**, *89*, 4733–4739.
(62) Sundholm, D. *Chem. Phys. Lett.* **1999**, *302*, 480–484.
(63) Sundholm, D. *Chem. Phys. Lett.* **2000**, *317*, 545–552.
(64) Cai, Z.-L.; Crossley, M. J.; Reimers, J. R.; Kobayashi, R.; Amos, R. D. *J. Phys. Chem. B* **2006**, *110*, 15624–15632.
(65) Marchanka, A.; Lubitz, W.; van Gastel, M. *J. Phys. Chem. B* **2009**, *113*, 6917–6927.

I−**V** and **VII** and **VIII** are slightly less negatively charged than in the respective basic structures. The effect is somewhat larger in **VI**, due to the coupling of the C-3 formyl (via oxygen lone pairs) with the π-electron system of the macrocycle. Both HOMO and LUMO energies in **I**−**IV** are by 0.10−0.16 eV lower than in the corresponding basic structure, while the energy gaps are approximately the same. Hence, their hardness is comparable, but their electronegativity varies from 4.23 (**II**) to 4.29 (**III**). Interestingly, in **V** and **VI** both HOMO and LUMO energies are shifted upward. While in **V** the HOMO−LUMO separation is smaller (1.54 eV) than in the other derivatives, in **VI** it is larger and amounts to 1.67 eV. In consequence, the electronegativities of **V** and **VI** remain similar, but their behavior may be dictated by the difference in their hardness which results from the presence of the side carbonyl group.

Both frontier orbitals in **VII** and **VIII** are shifted upward with respect to their energies in bare bacteriochlorin. The energy gap calculated for these species is considerably smaller than for **I**−**VI** and so is their hardness. This fact should be attributed to the properties of the basic macrocycle itself, as the same effect was also observed for chlorin and bacteriochlorin (Table 2).

Contribution of the π-Electron System to Porphyrinoid Reactivity. As discussed above, saturation of the tetrapyrrolic macrocycle is expected to essentially influence its reactivity in reactions with metal ions because it reduces ligand nucleophilicity. However, if reactions with very reactive metal ions, such as Zn^{2+}, are compared, then similar rates of metalation of porphyrins and pheophytins (**I**−**V**) indicate that the saturation of just one pyrrole ring has only a moderate influence on ligand reactivity. The effect is more pronounced when two pyrrole rings are reduced, causing very limited reactivity of **VII** and **VIII** in direct metalations. However, the effects of structural details on the chelating properties of free bases **I**−**VI** have to be related to the reactivity of the incoming metal ion. A good illustration of this is reactions with the Pt^{2+} ion, which requires strong activation and which, due to its inertness, is much more selective. Pt^{2+} insertion into **I** proceeds much faster than into a porphyrin under the same conditions,[19,57] and the differences between **I**−**VI** in the chelation of Pt^{2+} become striking: **IV** and **VI** are already much less reactive. Consequently, **VII** and **VIII** show no affinity toward Pt^{2+}.

The differences in the metalation rates of **I**−**VIII** cannot be easily explained in terms of the calculated charge distribution on the core nitrogens and the electronegativity of the tetrapyrrolic macrocycle. The charges accumulated on the nitrogens vary only slightly (in fact, the same holds for the entire set **I**−**VIII**), while the electronegativity is similar in porphyrin and 13^1-oxo-bacteriophorbin (~4.10) and increases to 4.35 in 13^1-oxo-phorbin, indicating their comparable capacity for electron donation and formation of coordination bonds. Somewhat clearer differences emerge when side chains are included in the modeling. The electronegativities of **I**−**IV** and **VIII** range near 4.25, while in **VII** this increases to 4.36 and to 4.45 in **V** and **VI**. However, again this order of electronegativity is not reflected in the metalation rate, especially with Pt^{2+}, and thus additional factors seem to determine the reactivity of the tetrapyrrolic π-electron system toward metallic centers. In particular, the very low reactivity of **VII** and **VIII** may result not from the electronegativities and the HOMO level in these ligands but may reflect the interplay between the low charge accumulated on the core nitrogens and a narrow energy gap.

Contribution of Peripheral Groups. C-7 Formyl. As **VI** is the least reactive among Chla derivatives toward both Zn^{2+} and Pt^{2+}, carbonyl in a peripheral position has the strongest influence on chelating capacity, among substituents of the tetrapyrrole macrocycle which vary in **I**−**VI**. Seemingly, the coupling of the formyl with the π-electron system in **VI** renders the core nitrogens less susceptible to electrophyllic attack,[66] in line with the fact that the side formyl group reduces the pK of the core nitrogens by about 2 units.[67] Several factors may contribute to this low reactivity of **VI** (and very likely of **VII** and **VIII** too): macrocycle flexibility and electronic effects. Many examples show that the rate of metal ion binding is related to the ability of porphyrin to distort from a planar conformation.[68−71] This is due to the fact that HOMOs and LUMOs are localized on the atoms constituting the macrocycle core (see above), and orbital energy-related properties, such as electronegativity and hardness, depend on the conformation of the macrocycle.[60] Although crystallographic studies on LHCII[72] show smaller conformational variability of the macrocycle of **VI**,[73] it is at present difficult to correlate it strictly with its flexibility. Instead, the electron-withdrawing ability of the formyl group, which originates from both the inductive (Hammett substituent constant $\sigma_m = 0.35$) and resonance effects, would be the major factor. A strong influence (coupling) of the C-7 carbonyl with the macrocycle π-electron system is obvious considering the shifts of the electronic transitions in **VI**. One may try to explain these lowered reaction rates for **VI** in the light of DFT calculations. Not only is its electronegativity high but also its HOMO energy is the highest. As the shapes of HOMOs are similar in all studied structures, it would be the HOMO energy in **VI** that determines its reactivity toward metal ions.

13^1-Oxo Isocyclic System. The present DFT calculations on the 13^1-oxo-phorbins show that the isocyclic ring V, a conservative structural element of all (B)Chls, does not affect the planarity of the tetrapyrrole. An extensive chlorin- or bacteriochlorin-based aromatic system must be more flexible than that of porphyrin,[74] but the isocyclic ring reduces this flexibility.[58,75] However, this is not

(66) Mazaki, H.; Watanabe, T.; Takahashi, T.; Struck, A.; Scheer, H. *Bull. Chem. Soc. Jpn.* **1992**, *65*, 3212–3214.
(67) Hoober, J. K.; Eggink, L. L. *FEBS Lett.* **2001**, *489*, 1–3.
(68) Lavallee, D. K. *The chemistry and biochemistry of N-substituted porphyrins*; Wiley-VCH: Weinheim, Germany, 1987; p 313.
(69) Bailey, S. L.; Hambright, P. *Inorg. Chim. Acta* **2003**, *344*, 43–48.
(70) Sigfridsson, E.; Ryde, U. *J. Biol. Inorg. Chem.* **2003**, *8*, 273–282.
(71) Al-Karadaghi, S.; Franco, R.; Hansson, M.; Shelnutt, J. A.; Isaya, G.; Ferreira, G. C. *Trends Biochem. Sci.* **2006**, *31*, 135–142.
(72) Liu, Z.; Yan, H.; Wang, K.; Kuang, T.; Jiping, Z.; Gui, L.; An, X.; Chang, W. *Nature* **2004**, *428*, 287–292.
(73) Zucchelli, G.; Brogioli, D.; Casazza, A. P.; Garlaschi, F. M.; Jennings, R. C. *Biophys. J.* **2007**, *93*, 2240–2254.
(74) Senge, M. O. Highly substituted porphyrins. In *The Porphyrin Handbook*; Kadish, K. M., Smith, K. M., Guilard, R., Eds.; Academic Press: Amsterdam, The Netherlands, 1999; Vol. *1*, pp 239−347.
(75) Petke, J. D.; Maggiora, G. M.; Shipman, L. L.; Christoffersen, R. E. *Photochem. Photobiol.* **1979**, *30*, 203–223.

necessarily translated into any decreased chelating capacity of Chls. As discussed above, plane porphyrin and **I** show very similar reactivity toward Pt^{2+} and Zn^{2+} ions. Another clear effect seems to be related to the presence of oxo-substituent and methoxycarbonyl at the C-13[1] and -13[2] positions, respectively, which facilitates the keto−enol tautomerism in the isocyclic ring. As mentioned, this tautomeric system affects the acetate-assisted metal insertion in **VII**[15] and the transmetalation of Chla.[33] In the present experimental system of neutral solvents (see above), there are no significant differences in metal insertion into free base **I** and into its analogs (**III** and **V**), which lacks a tautomerizable system at the isocyclic ring. The influence of keto−enol tautomerism seems much more pronounced in metal exchange.[33]

Phytyl. The bulky phytyl moiety is involved in steric interactions around rings IV and V in Chl and BChl which affects core nitrogens in their interactions with H-bond donors and increases the rigidity of the macrocycle.[24,31,32] Also the present DFT calculations show the involvement of phytyl in these types of steric interactions (see above). Because conformational effects are among the chief reactivity determinants for porphyrins,[25,68] the removal of this residue might be expected to facilitate metalation. Nevertheless, the rate of Zn^{2+} insertion in **IV** in MeCN is visibly lower than that of the phytylated derivatives **I**−**II** and **V** (Table 1), and a similar effect is observed in the insertion of the Pt^{2+} ion (30 min at 80 °C for **I** vs 100 min at 95 °C for **IV**). This deactivation of **IV** cannot to be easily attributed to the electron-withdrawing ability of the free carboxyl because the Hammett parameter σ_m (0.035) of this functionality is identical to that of an ester group. Possibly, it is related to a local effect of free carboxyl, which is capable of proton donation to the core nitrogens which then inhibits metal insertion, or is caused by electrostatic repulsion of the incoming metal ion when the carboxyl binds a metal ion (used in excess in the experiment). This is in line with the fact that there are no differences in the reactivity of **I**−**V** in MeOH, which is both weakly H-bonding and strongly coordinating.

Relevance to Biological Metal Insertion. It is accepted that chelatase action involves a distortion of the tetrapyrrole macrocycle, the abstraction of two protons from the substrate, and the exposure of the core nitrogens to the incoming metal ion.[71] The distortion of the tetrapyrrolic ligand seems not only to enhance the reaction rate by decreasing the activation energy of the process but also to partly determine which divalent metal ion is to be incorporated.[71,76,77] However, a general mechanism accounting for chelatase selectivity toward metal ions is not well established.[78,79] For instance, ferrochelatase catalyzes (in vitro) the insertion of several types of divalent metal ions into PPIX.[78] Recently, however, it became clear that this metal selectivity of ferrochelatase observed in vitro is an artifact of slow product release and most likely is not relevant in vivo.[80,81] On the other hand, magnesium chelatase is highly specific for Mg^{2+} and excludes even metal ions closely related to Mg, such as Zn^{2+}.[79] In this respect, the catalytic activity and selectivity of Mg-chelatase is intriguing because from a synthetic point of view the insertion of Mg^{2+} is rather troublesome,[35] whereas the transmetalation of Chls with many other divalent metal ions (e.g., Zn, Cu, Ni, and Co) occurs spontaneously in vitro and in vivo.[12−14,34] Also it remains unclear how other structural and electronic factors affect the enzymatic metalation of tetrapyrroles. Theoretical studies show that the formation of a metal-core nitrogen bond is facilitated by dehydration and a stepwise decrease in the coordination number of the Fe(II) ion upon binding to ferrochelatase. These studies also indicate a need for the assistance of amino acid residues in proton removal.[82] Perhaps two side propionates, which seem to interact with active site residues via hydrogen and ionic bonds to ensure a highly specific spatial orientation of the porphyrin in the active site, are involved in the dehydration of the incoming Fe(II).[76] Also a cooperative binding model has been considered, in which residues from both the N- and C-terminal regions are involved in binding the PPIX molecule which in turn induces a conformational change where the thumb and finger subdomains of the enzyme fuse.[83]

The present experimental and theoretical analysis provides new insights into the understanding of mechanism of metal insertion catalyzed by chelatases. It points at several additional factors which are relevant to the mechanism of chelatase catalysis, as they determine the chelating properties of tetrapyrroles. First, the coordination/solvation by solvent and the activation of inert metal ions, such as Mg^{2+}, crucially affect the kinetics of metal insertion into tetrapyrrolic ligands. The necessity for the activation of the Mg^{2+} ion was evidenced in a recent study, which showed a very high energetic demand, up to 15 ATP molecules, for reactions mediated by magnesium chelatase.[84] On the other hand, our previous study showed a significant involvement of carboxylic groups in the catalysis of metal insertion into Chls,[33] suggesting possible participation of glutamic and aspartic acid side carboxyls in the catalytic cycle of chelatases. Furthermore, both the DFT calculations and experimental results show the strong influence of the macrocycle rigidity and of peripheral groups on the chelating ability of Chls. In particular, the peripheral functionalization seems to drastically reduce its reactivity toward metal ions. The effect of peripheral groups is at least two-fold: (i) a lower electron density on the core nitrogens, and (ii) an increased rigidity of the macrocycle. These effects seem less relevant for the insertion of Fe(II) during heme biosynthesis but are important for Mg^{2+} insertion as they provide a rationale for why it takes place at an early stage of (B)Chl biosynthesis, before other

(76) Medlock, A.; Swartz, L.; Dailey, T. A.; Dailey, H. A.; Lanzilotta, W. N. *P. Natl. Acad. Sci. U.S.A.* **2007**, *104*, 1789–1793.
(77) Hansson, M. D.; Karlberg, T.; Rahardja, M. A.; Al-Karadaghi, S.; Hansson, M. *Biochemistry* **2007**, *46*, 87–94.
(78) Masuda, T.; Inoue, K.; Masuda, M.; Nagayama, M.; Tamaki, A.; Ohta, H.; Shimada, H.; Takamiya, K. I. *J. Biol. Chem.* **1999**, *274*, 33594–33600.
(79) Rüdiger, W. *Photosynth. Res.* **2002**, *74*, 187–193.
(80) Davidson, R. E.; Chesters, C. J.; Reid, J. D. *J. Biol. Chem.* **2009**, *284*, 33795–33799.
(81) Medlock, A.; Carter, M.; Dailey, T. A.; Dailey, H. A.; Lanzilotta, W. N. *J. Mol. Biol.* **2009**, *393*, 308–319.
(82) Shen, Y.; Ryde, U. *Chem.—Eur. J.* **2005**, *11*, 1549–1564.
(83) Sirijovski, N.; Lundqvist, J.; Rosenbäck, M.; Elmlund, H.; Al-Karadaghi, S.; Willows, R. D.; Hansson, M. *J. Biol. Chem.* **2008**, *283*, 11652–11660.
(84) Reid, J. D.; Hunter, C. N. *J. Biol. Chem.* **2004**, *279*, 26893–26899.

functional groups are being attached at the periphery of the macrocycle. Seemingly, Mg^{2+} insertion at these further stages would become biosynthetically even more difficult.

Conclusions

The present systematic study reveals how various structural features project on the chelating properties of porphyrinoids, both the degree of macrocycle oxidation and peripheral groups, in particular carbonyls, suppress the reactivity. In terms of the incoming metal ion, solvent properties are the most decisive. The results of the DFT calculations show that porphyrinoid reactivity in metalation reactions is a rather complicated interplay of many factors. There are only slight variations in chemical hardness, electronegativity, and the HOMO energy along the porphyrin−chlorophyll−bacteriochlorophyll row, and thus these reactivity descriptors do not determine the chelating properties in the row. The reactivity order seems better correlated with decreasing charge densities on nitrogens (Loewdin charges) and with decreasing HOMO−LUMO gaps in the row. The reactivity of the core nitrogens is also reduced when carbonyls are present at the macrocycle periphery. Carbonyl groups not only have electron-withdrawing properties but strongly conjugate to porphyrinoid π-electron system and render the macrocycle more rigid.

The present experimental (kinetics of metalation) and theoretical analysis (static reactivity descriptors of porphyrinoids) provides new insights into the understanding of mechanism of metal insertion catalyzed by chelatases. First, the activation of inert metal ions, such as Mg^{2+}, by the enzyme is at least as important as the macrocycle activation. Second, as the macrocycle reduction and the peripheral functionalization lead to a drastic lowering of porphyrinoid reactivity toward metal ions, Mg^{2+} insertion in (B)Chl biosynthetic pathway must take place before the chlorin and bacteriochlorin formation and any further derivatization.

Acknowledgment. The work was supported by the Polish Ministry of Science and Higher Education (Grants no. PB 1505/P01/2007/32 and R 05 043 03). The Faculty of Biochemistry, Biophysics, and Biotechnology and the Faculty of Chemistry of the Jagiellonian University are the beneficiaries of the structural funds from the European Union (grants no. POIG.02.01.00-12-064/08 "Molecular biotechnology for health" and no. POIG. 02.01.00-12-023/08 "Atomic Scale Science for Innovative Economy (ATOMIN)", respectively).

Supporting Information Available: Spectral changes accompanying the reactions of free base porphyrinoids with Zn^{2+} ions. This material is available free of charge via the Internet at http://pubs.acs.org